Title: Critical role of PP2A-B56 family protein degradation in HIV-1 Vif mediated G2 cell cycle arrest

Author names:

Kayoko Nagata, Keisuke Shindo, Yusuke Matsui, Kotaro Shirakawa and Akifumi Takaori-Kondo

Affiliation:

Department of Hematology and Oncology, Graduate School of Medicine, Kyoto University

Correspondence

Keisuke Shindo, Department of Hematology and Oncology, Graduate School of Medicine, Kyoto University, 54 Shogoin-Kawaracho, Sakyo-ku, Kyoto, 606-8507, Japan.

E-mail: shind009@kuhp.kyoto-u.ac.jp

Abstract

HIV-1 Vif forms an E3 ubiquitin ligase complex with host proteins to counteract host restrictive APOBEC3, and is also known to accumulate infected cells at the G2 phase to promote viral replication. However, the underlying mechanism of how Vif induces G2 arrest is not fully understood, and more specifically, direct target molecules of G2 arrest have not been identified. Here we show that degradation of B56 family proteins (PP2A-B56), one of the regulatory subunits of protein phosphatase 2A, is critical for the Vif-induced G2 arrest. NL4-3 Vif caused degradation of PP2A-B56, and complementation of PP2A-B56 overcome the Vif-induced arrest. Supportively, knockdown of PPP2R5D, one of PP2A-B56, by siRNA itself induced cell cycle arrest of non-infected cells. We also identified Vif residues I31 and R or K33 are determinants for inducing G2 arrest, and Vif variants that did not cause G2 arrest did not induce PPP2R5D degradation, although it maintain the ability to induce APOBEC3G degradation, showing strong correlation between Vif-induced arrest and PP2A-B56 degradation. In a sequence database of HIV-1 isolates, Vif strains harboring residues that presumably induce cell cycle arrest are approximately 43%, suggesting Vif-induced G2 arrest contributes to HIV-1 infection *in vivo* and spread. Our data help understand the mechanism of Vif-mediated arrest, and gain insights into general cell cycle regulation.

Keywords: Virion infectivity factor, PP2A, HIV-1, cell cycle arrest, ubiquitination

Introduction

Viruses modify intracellular environment of infected cells in several ways, and cell cycle alteration is one such way for several viruses. HIV-1 infection is also known to cause accumulation of infected cells at G2 phase. The transcription of the HIV-1 long terminal repeat is very high during the G2 phase in HIV-1 infected cells, resulting in efficient viral replication [1], therefore intracellular environment during the G2 phase of HIV-1 infected cells is thought to be optimized for viral replication. This cell cycle arrest by HIV-1 has long been attributed to the function of an accessory protein Vpr, and several groups reported the molecular mechanism of Vpr-induced cell cycle arrest. However, since HIV-1 with loss-of-function mutants of Vpr also caused G2 arrest, the involvement of another viral protein was suggested. The mutant of HIV-1 that both vpr and vif genes were deleted is incapable of inducing G2 arrest [2], and the expression of Vif alone is sufficient for G2 arrest [3], indicating the invlovement of Vif in G2 arrest. HIV-1 Vif forms a complex with the E3 ubiquitin ligase complex comprising cellular proteins, cullin-5, elongin B, elongin C, RING-box protein 2 and a transcriptional co-activator, CBFβ. The resulting Vif-E3 ligase complex targets a host antiviral defense protein APOBEC3, and induces its degradation through the ubiquitin-dependent proteasome pathway, leading to the enhancement of HIV-1 replication [4,5]. The same Vif-E3 ligase complex is required for G2 arrest [6]. Interestingly, The variants of Vif such as NL4-3 Vif causes cell cycle arrest, but HXB2 Vif does not [7,8]. However, a direct target molecule for the Vif-mediated arrest has not been identified.

Recently, a proteome analysis of the HIV-1 infected cells has identified B56 family proteins of PP2A B subunit, PPP2R5A-E, as novel substrates of the Vif-E3 ligase complex [9]. PP2A is a hetero-trimeric holoenzyme comprising three subunits; B (regulatory) subunit defines the substrate selectivity, while A (scaffold) and C (catalytic) subunits form the core enzyme. B subunit proteins are classified into four subfamilies according to their amino acid sequence similarity: PR55, B56, PR72, and Striatin [10]. Although the functions of PP2A-B56 are largely unknown, based on the evidence that another family of PP2A B subunit, PP2A-PR55, play roles as a negative regulator of cell cycle, we hypothesized that the degradation of the PP2A-B56 may be one of the key events in the Vif-mediated G2 arrest. Here, we report PP2A-B56 are the direct target for the Vif-mediated arrest. Moreover, we demonstrate that NL4-3 Vif-induced arrest is suppressed by the overexpression of each of the five PP2A-B56 members, while the G2 cell cycle arrest of the non-infected cells are induced by the siRNA inhibition of PPP2R5D in 293T cells. Additionally, we confirm that I31 and R33 residues of NL4-3 Vif are involved in the binding of PPP2R5D, and by substitution of these residues, we demonstrate the strong correlation between PPP2R5D degradation and G2 arrest. Our data establish the critical role of PP2A-B56 degradation in the HIV-1 Vif-mediated arrest, and provide additional information on general regulation of the cell cycle.

Material and methods

Cell culture

293T cells were cultured in Dulbecco's modified Eagle's medium (Nacalai Tesque, Japan) supplemented with 10% fetal bovine serum (FBS, Gibco) and penicillin, streptomycin, and glutamine (PSG, Gibco). CEM-SS cells were cultured in RPMI1640 medium (Nacalai) supplemented with 10% FBS and PSG.

Plasmid construction

Firstly, oligonucleotides 5'-GATCAAGATCTATCGATGCGGCCGCAGGATCCG-3' and 5'-TCGACGGATCCTGCGGCCGCATCGATAGATCTT-3' (Fasmac) were annealed and inserted into pDON-AI (Takara) at *Bam*HI/*Sal*I sites to introduce additional restriction sites, *Bgl*II, *Cla*I, *Not*I, *Bam*HI, and *Sal*I, and resulting plasmid was named pDON-AI-MCS2. Secondly, the *IRES-GFP* gene was cleaved out from the pCSII-CMV-MCS-IRES-hrGFP using *Not*I and *Hpa*I, and inserted into pDON-AI-MCS2 at *Not*I/*Hpa*I sites. The generated plasmid was named pDON-AI-IRES-GFP. Thirdly, each of the coding sequences for NL4-3 Vif and its various mutants was amplified by polymerase chain reaction (PCR) and inserted into the pDON-AI-IRES-GFP, individually. Expression plasmids for PPP2R5A, PPP2R5B, PPP2R5C-myc, PPP2R5D-myc, and PPP2R5E were produced by amplifying their coding sequences by PCR and inserted into pcDNA3 (Invitrogen), individually. The Flag-tagged ubiquitin expression plasmid was previously described [7].

Transfection and virus infection

For cell cycle analysis, 293T cells were transfected by using Calphos mammalian transfection kit (Clontech) according to the manufacturer's instructions. For immunoprecipitation, 293T cells were transfected by using X-tremegene HP DNA transfection reagent (Roche) according to the manufacturer's instructions. For retrovirus preparation, 293T cells were transfected using polyethyleneimine (PEI) at a PEI: DNA ratio of 2.25: 1 (w: w). Forty-eight hours after transfection, virus-containing supernatants were harvested through the 0.45 μm pore-sized PVDF filter, and subsequently concentrated by ultracentrifugation. CEM-SS cells were then inoculated with the concentrated virus for 72 h.

Immunoblotting

For immunoblotting, we used a general chemiluminescence protocol with PVDF membrane (Millipore). Following primary antibodies were used: anti-Vif, anti-PPP2R5A, anti-PPP2R5B, anti-PPP2R5C, anti-PPP2R5D, and anti-PPP2R5E (Santa Cruz); anti-β-actin, anti-c-Myc, and anti-Flag (Sigma-Aldrich); anti-A3G (NIH AIDS Reagent Program).

Cell cycle analysis

To detect cell cycle arrest, DNA contents of transfected 293T cells and infected CEM-SS cells were examined using flow cytometry. Either 48 h after transfection or 72 h after infection, cells were harvested,

104 washed with PBS, and then fixed in ice-cold 70% ethanol at 4ºC. Cells were then washed with 2% FBS/PBS,
105 stained with propidium iodide (Nacalai) at 10 μg/ml containing 200 μg/ml RNase A (QIAGEN) and 2%
106 FBS/PBS at 37ºC, and examined on a FACSCalibur flow cytometer (Becton Dickinson). Data were
107 analyzed with Flowjo software.
108
109 *Co-immunoprecipitation*
110 Transfected 293T cells were treated with MG132 (Calbiochem) at 2.5 μM for 16 h, and lysed with co-IP
111 buffer (50 mM Tris pH8.0, 250 mM NaCl, 5 mM EDTA, and 0.3% CHAPS) supplemented with protease
112 inhibitor cocktail (Roche) and 50 μM MG132. Lysates were immunoprecipitated with anti-myc antibody
113 for 3 h at 4ºC, and then mixed with protein A or G sepharose beads (GE Healthcare) for 2 h. Beads were
114 washed with co-IP buffer, and bound proteins were eluted and analyzed by immunoblotting.
115
116 **Results**
117
118 *The formation of the Vif-E3 ligase complex is required for the Vif-induced cell cycle arrest*
119
120 Previous studies on Vif-mediated arrest utilized fluorescent protein to extract Vif-expressing cells by co-
121 transfection [8] or fusion protein [7]. These approaches were basically successful, however, substitutional

analyses of Vif amino acid residues sometimes caused inconsistent results, because of the low efficiency of arrest induction. To analyze the Vif-induced arrest more sensitively, we successfully took advantage of IRES-containing expression vector that simultaneously expresses Vif and EGFP proteins. By using this vector in 293T cells, the ratio of Vif-expressing cells at G2/M phase over those at G1 phase increased to around two, whereas that of empty-vector-transfected cells remained around 0.7 (Supplementary Figures 1C and 1D). We first aimed to confirm the previous report that the formation of the Vif-E3 ligase complex is required for the Vif-mediated arrest [6]. We generated three kinds of Vif amino acid substitutions C133S [4], ^{144}SLQ^{146}/AAA [11,12], and E88A/W89A [13], into the Vif-IRES-EGFP vector (Supplementary Figure 1A). All these Vif mutants do not form functional E3 ligase complex, therefore are incapable of degrading APOBEC3G (Supplementary Figure 1B). We then performed cell cycle analysis on 293T cells using these vectors. The cell number in the G2/M phase was remarkably increased by expressing Vif wild-type, but not by any of the Vif mutants tested (Supplementary Figures 1C and 1D), indicating that the formation of the Vif-E3 ligase complex is required for G2 arrest.

PP2A-B56 are substrates for the Vif-E3 ligase complex and affect cell cycle progression

A proteomic approach has recently identified that the members of PP2A-B56, including PPP2R5A, B, C, D, and E, are substrates of the Vif-E3 ligase complex [9]. We next examined whether Vif-induced

degradation of PP2A-B56 is related to the Vif-induced arrest. To confirm that PP2A-B56 are degraded by Vif, 293T cells were transfected with the expression vector for NL4-3 Vif, HXB2 Vif, SLQ mutant, or empty vector, and then PP2A-B56 levels were analyzed by immunoblotting. Of note, NL4-3 Vif is capable of inducing G2 arrest, but HXB2 Vif is not [7]. PPP2R5A level in the cells expressing either NL4-3 Vif or HXB2 Vif was lower than that in the cells transfected with the empty vector or SLQ mutant, while the levels of PPP2R5B, C, and E were not clearly determined because of low endogenous expression levels (Figure 1A). Interestingly, PPP2R5D level in the cells expressing NL4-3 Vif was lower than that in the cells expressing either HXB2 Vif or SLQ mutant, or that in the cells with the empty vector (Figure 1A). We next examined whether exogenously expressed PP2A-B56 are degraded by Vif. Each of PP2A-B56 expression vector is co-transfected with the expression vector for NL4-3 Vif, or empty vector, then PP2A-B56 levels were analyzed. The levels of PPP2R5A, B, C, D, and E in NL4-3 Vif expressing cells were lower than those in empty vector transfected cells (Figure 2B). These results indicate that all of PP2A-B56 are substrates of the NL4-3 Vif-E3 ligase, consistent with the previous report. Because the downregulation of endogenous PPP2R5D was most clearly observed in 293T cells, we used PPP2R5D as a prototype to confirm the relationship between PP2A-B56 degradation and the Vif-mediated arrest in 293T cells.

We further confirmed that PPP2R5D is a substrate of the Vif-E3 ubiquitin ligase complex. Treatment of MG132, a proteasome inhibitor, restored the level of PPP2R5D downregulated by Vif expression (Supplementary Figure 2A). Interaction between Vif and PPP2R5D was confirmed by co-

158 immunoprecipitation experiments (Supplementary Figure 2B). Additionally, poly-ubiquitination of
159 PPP2R5D in the Vif expressing cells was higher than that in empty vector transfected cells (Supplementary
160 Figure 2C). Altogether, these results support that PPP2R5D is a substrate of Vif-E3 ligase complex.

161 We next performed complementation experiments. If the degradation of PPP2R5D is required for
162 the Vif-mediated arrest, complementation of PPP2R5D by co-transfection would counteract G2 arrest. 293T
163 cells were co-transfected with the expression vectors for Vif and one of PP2A-B56 and cell cycles were
164 analyzed. Consistent with our expectation, co-expression of Vif and PPP2R5D did not induce G2 arrest.
165 Surprisingly, co-expression of Vif and PP2R5A, B, C, or E also did not induce G2 arrest (Figures 1C and
166 1D), suggesting that all of PP2A-B56 family members individually work in counteracting the Vif-induced
167 arrest.

168 Additionally, to investigate whether down-regulation of PPP2R5D is sufficient to induce cell
169 cycle arrest, we performed knockdown experiments of PPP2R5D. 293T cells were transfected with one of
170 two different siRNAs targeting PPP2R5D [siPPP2R5D (878) and siPPP2R5D (939)], or non-silencing
171 control RNA. The efficiency of the knockdown was analyzed by immunoblotting (Figure 1E). We then
172 analyzed these cells for cell cycle, and found accumulation of cells at G2/M phase (Figures 1F and 1G),
173 suggesting that targeting of PPP2R5D alone for degradation is sufficient for cell cycle arrest in 293T cells.

174

175 *I31 and R33 residues of NL4-3 Vif are critical for the PPP2R5D degradation*

To further examine the correlation between Vif-induced arrest and PPP2R5D degradation, we next aimed to identify Vif residues that recognize PPP2R5D. A couple of previous studies of amino acid substitution between NL4-3 Vif and HXB2 Vif have identified six residues, I31, R33, K36, Y47, H48 and K50, as Vif determinants for G2 arrest [7,8] (Figure 2A). We expressed six NL4-3 Vif mutants, I31V/R33G/K36R, I31V, R33G, K36R, T47P/K50R, and H48N, individually, in 293T cells and analyzed their effects on cell cycle. Consistent with the previous report, I31V/R33G/K36R, I31V, or R33G did not induce G2 arrest, however, K36R, T47P/K50R, and N48H appeared to induce G2 arrest to some extent (Figures 2B and 2C). These results indicate that I31 and R33 residues of NL4-3 Vif are critical for the Vif-induced arrest. We then examined protein levels of PPP2R5D in the cells expressing each of the Vif mutants by immunoblotting. PPP2R5D decreased in the cells expressing Vif wild-type, K36R, T47P/K50R, or N48H, but not in the cells expressing I31V/R33G/K36R, I31V or R33G (Figure 2D). To exclude the possibility that these mutants do not form the functional Vif-E3 ligase complex, APOBEC3G degradation was examined. All of the Vif mutants definitely induced APOBEC3G degradation (Figure 2E), indicating that these Vif mutants work as an E3 ubiquitin ligase.

Considering that I31V and R33G induced APOBEC3G degradation, but not PPP2R5D degradation, Vif I31 and R33 might interact with PPP2R5D. To examine this possibility, we performed co-immunoprecipitation experiments with Vif I31V/R33G. The amount of PPP2R5D co-precipitated with

myc-tagged Vif I31V/R33G appeared to be lower than that co-precipitated with myc-tagged Vif wild-type (Figure 2F), suggesting that the residues I31 and R33 are involved in PPP2R5D binding. Altogether, these results indicate that the Vif-mediated arrest and PPP2R5D degradation strongly correlates, and that the residues I31 and R33 of NL4-3 Vif play the central role in the PPP2R5D recognition.

Vif variants harboring K33 is capable of inducing the cell cycle arrest

So far, we examined Vif residues based on amino acid sequences of NL4-3 Vif and HXB2 Vif. According to the HIV-1 sequence database by Los Alamos National Laboratory (LANL, http://www.hiv.lanl.gov/content/sequence/HIV/mainpage.html), isoleucine (NL4-3) and valine (HXB2) are two major residues for Vif position 31, but lysin, not arginine (NL4-3) or glycine (HXB2), is the most frequent residue for position 33 (Figure 3A). To examine whether Vif variants harboring K33 induce G2 arrest, we expressed NL4-3 Vif R33K in 293T cells, and analyzed its effect on cell cycle. Interestingly, Vif R33K induced G2 arrest of transfected cells comparably to NL4-3 Vif wild-type (Figure 3B). PPP2R5D degradation by Vif R33K was confirmed by immunoblotting (Figure 3C), consistent with the idea that PPP2R5D degradation is relevant to the Vif-mediated arrest. APOBEC3G was also downregulated by Vif R33K (Figure 3D). To speculate contributions of Vif residues other than I31 and R/K33 to Vif-mediated arrest, we generated expression vectors for HXB2 Vif V31I/G33R and V31I/G33K mutants. Both of these

mutants strongly induced G2 arrest (Figure 3E), and degradation of PPP2R5D (Figure 3F) and APOBEC3G (Figure 3G), suggesting little contributions of other residues to PPP2R5D recognition. Taken together, Vif strains harboring I31 and R/K33, which consist of the majority of isolated strains, are likely to induce G2 arrest.

PP2A-B56 degradation is relevant to HIV-1 Vif-induced arrest in T cells

To confirm our findings in more physiological condition, we used a T cell line in which HIV-1 can replicate. We examined endogenous levels of PP2A-B56 and their degradation by Vif in CEM-SS cells. CEM-SS cells were retrovirally transduced with NL4-3 Vif, HXB2 Vif, or empty vector, and then PP2A-B56 levels were analyzed by immunoblotting (Figure 4A). PPP2R5A was degraded by either NL4-3 Vif or HXB2 Vif, while PPP2R5D were degraded only by NL4-3 Vif, similarly to the results obtained with 293T cells. The endogenous PPP2R5B and C in CEM-SS cells were not detected by immunoblotting. Apart from the results with 293T cells, endogenous PPP2R5E was clearly detected in CEM-SS cells, and degraded by NL4-3 Vif, but not by HXB2 Vif. We next examined whether overexpression of PP2A-B56 counteracts to Vif-mediated arrest. CEM-SS cells were transduced with NL4-3 Vif and PPP2R5C, D, E, or empty vector, and cell cycle were analyzed (Figure 4B). Transduction of NL4-3 Vif accumulated the cells at G2/M phase, and co-transduction of PPP2R5D or E with NL4-3 Vif significantly decreased cells at G2/M phase, compared to Vif-transduced cells. Co-transduction of

PPP2R5C with NL4-3 Vif into CEM-SS cells appeared to slightly decrease cells at G2/M phase, compared to Vif-transduced cells, because of weak expression of PPP2R5C (Figure 4C). All of these results from CEM-SS cells are very similar to those in 293T cells (Figure 1). We further examined the potency of Vif mutants for cell cycle arrest induction and PPP2R5D degradation in CEM-SS cells. NL4-3 Vif R33K, N48H, and T47P/K50R induced G2 arrest in CEM-SS cells comparably to NL4-3 Vif wild-type, but I31V/R33G did not (Figure 4D). PPP2R5D protein levels were simultaneously analyzed by immunoblotting, and down-regulated by NL4-3 Vif wild-type, R33K, N48H, and T47P/K50R, but not by I31V/R33G (Figure 4E). All of the data obtained in CEM-SS cells were similar to the result with 293T cells (Figures 2 and 3). Thus, our finding that PP2A-B56 degradation by Vif is relevant to Vif-mediated arrest is likely true in T cells.

Discussion

We here demonstrate that PP2A-B56 family proteins are the direct targets of Vif-mediated G2 arrest, and that PPP2R5D is most likely to be relevant to G2 arrest in 293T cells. PP2A has been reported to play important roles in the regulation of cell cycle. Basically G2/M transition is regulated by the Cdc25/14-3-3 interaction; Dephosphorylation at Ser-218 of Cdc25 triggers its dissociation from 14-3-3 leading to the activation of Cdc25, resulting in G2/M transition. Phosphatases such as PP-1 and PP2A work as a positive regulator in this dephosphorylation. On the other hands, PPP2R5D is shown to play a different role in this

step; It dephosphorylates active phosphorylation at Thr-130 of Cdc25, working as a negative regulator[14]. Thus, it is quite complicated to evaluate the precise role of PP2A-B56 in the cell cycle regulation.

Recently, Salamango *et al*. reported that combinatory suppression of two of PPP2R5A, C, or D causes cell cycle arrest in 293T cells, which are the target of Vif-induced degradation [15]. Their finding is partially different from ours that suppression of PPP2R5D alone is sufficient for G2 arrest. Since we showed that each PP2A-B56 is expressed at different levels depending on cell types, this discrepancy might be attributable to different expression profiles of PP2A-B56 in different cell types. Moreover, we show that complementation of each of the PP2A-B56 overcame the Vif-induced G2 arrest, proving direct relation between Vif-induced arrest and PP2A-B56 degradation.

In this study, we clearly demonstrated that NL4-3 Vif I31 and R33 residues are critical for the Vif-mediated arrest and PPP2R5D degradation, but either K36, T47, N48 or K50 is not, supporting the correlation between PPP2R5D degradation and the Vif-mediated arrest. We further elucidated that a major variant K33 is capable of inducing G2 arrest. According to the HIV-1 sequence database by LANL, conservation of both I31 and R/K33 residues of Vif was about 43% (1919/4465). In contrast, according to the reports analyzing the gene sequence of Vif in HIV-1 infected patients, the Vif harboring both I31 and R/K33 was found to be 72% (76/105) in North India [16], 23% (6/26) in South Africa [17], and 48% (37/77) in Mexico [18]. Thus, the frequency of Vif harboring I31and R/K33 in HIV-1 infected patients varies among regions, but Vif-mediated arrest would happen in the majority of patients with HIV-1 infection, and could

be advantageous to HIV-1 infection *in vivo* and spread.

We demonstrate that PP2A-B56 are substrate of the majority of HIV-1 Vif strains, and the degradation of PPP2R5D is closely related to Vif-mediated arrest. Our data suggest that PP2A-B56 might play roles in the regulation of the cell cycle through phosphorylation-based signal transduction. Further studies on the Vif-mediated arrest will contribute to elucidate profound regulatory system of the cell cycle.

Acknowledgments

We thank the laboratory members for helpful discussion. We also thank Dr. Takashi Nagata in Institute of Advanced Energy, Kyoto University for critical reading. Anti-human APOBEC3G C-terminal serum was obtained from Dr. Jaisri Lingappa through the NIH AIDS Reagent Program, Division of AIDS, NIAID, NIH. This work was partly supported by grants-in-aid for scientific research from Japan Society for the Promotion of Science (KAKENHI #JP 16K08807 to Shindo).

Figure Legends

Figure 1. PP2A-B56 are substrates for the NL4-3 Vif-E3 ligase complex and effect on cell cycle progression.

(A) Downregulation of PPP2R5D by NL4-3 Vif overexpression. 293T cells were transfected with expression vector for NL4-3 Vif, HXB2 Vif, SLQ mutant, or empty vector (EV), and analyzed for protein levels of endogenous PPP2R5A-E by immunoblotting. Asterisk indicate non-specific signal. (B) Overexpressed PP2A-B56 are downregulated by NL4-3 Vif. 293T cells were co-transfected with expression vectors for each of PP2A-B56 and Vif, and analyzed for PPP2R5A-E levels by immunoblotting. (C) Representative histogram for 293T cells co-transfected with each of PP2A-B56 and Vif. Cells at G1, S, and G2/M phase are colored in *blue*, *yellow*, and *green*, respectively. (D) Bar chart represents the (G2+M)/G1 ratios from three independent experiments in (C). Asterisks indicate statistical significances (*: $P<0.05$, **: $P<0.01$). (E) Validation of two different siRNA against PPP2R5D. 293T cells were transfected with either non-silencing control RNA, siPPP2R5D (878), or siPPP2R5D (939), and the PPP2R5D protein levels were analyzed by immunoblotting. (F) Representative histogram for 293T cells transfected with each of the two different PPP2R5D siRNAs. (G) Bar chart represents the (G2+M)/G1 ratios from three independent experiments in (F). Asterisks indicate statistical significances (**: $P<0.01$).

Figure 2. Identification of Vif residues involved in the recognition of PPP2R5D. (A) Protein sequence alignment of the N-terminal regions of NL4-3 Vif and HXB2 Vif. The residues of HXB2 Vif that are conserved with NL4-3 Vif are indicated by asterisk. (B) Representative histogram for 293T cells transfected with indicated vectors. (C) Bar chart represents the (G2+M)/G1 ratios from three independent experiments

in (B). Asterisks indicate statistical significances (*: P<0.05, **: P<0.01). (D) PPP2R5D levels in the cells studied in (B) were analyzed by immunoblotting. (E) Validation of ubiquitin ligase activity of Vif mutants against APOBEC3G. 293T cells were transfected with the expression vector for APOBEC3G and the indicated vector for Vif wild type (WT), mutants, or EV, and the levels of indicated proteins were analyzed by immunoblotting. (F) Impaired co-immunoprecipitation of PPP2R5D with Vif I31V/R33G mutant. 293T cells were transfected with indicated vectors (myc-tagged Vif WT, I31V/R33G, or EV), immunoprecipitated with anti-myc antibody for Vif proteins, and bound proteins were analyzed by immunoblotting.

Figure 3. A major variant of HIV-1Vif is capable of inducing cell cycle arrest. (A) An alignment of HIV-1 Vif residues 30 to 50. A sequence logo based on the database by LANL and NL4-3 and HXB2 Vif sequence were aligned. (B) Representative histogram for 293T cells transfected with indicated vectors. (C) Immunoblotting analyses of cells in (B). (D) Immunoblotting analyses of APOBEC3G degradation by Vif R33K. (E) Representative histogram for 293T cells transfected with indicated vectors. (F) Immunoblotting analyses of cells in (E). (G) Immunoblotting analyses of APOBEC3G degradation by HXB2 Vif wild-type and mutants.

Figure 4. Correlation between PP2A-B56 degradation and Vif-induced arrest in T cells. (A) Immunoblotting

analysis of endogenous PP2A-B56 protein levels in CEM-SS cells. CEM-SS cells were infected with indicated viruses and analyzed for PP2A-B56 levels by immunoblotting. (B) Complementation of PPP2R5C, D or E impairs Vif-induced arrest in CEM-SS cells. CEM-SS cells were infected with indicated viruses and the cell cycle distribution was analyzed. (C) Immunoblotting analysis of PP2A-B56 protein levels in CEM-SS cells infected with viruses transducing Vif and PP2A-B56. (D) I31 and R/K33 are critical for Vif to induce G2 arrest. CEM-SS cells were infected with indicated viruses and the cell cycle distribution was analyzed. (E) Immunoblotting analyses of the cells in (D).

References

[1] M. Emerman, HIV-1, Vpr and the cell cycle, Curr Biol 6 (1996) 1096-1103.

[2] K. Sakai, J. Dimas, M.J. Lenardo, The Vif and Vpr accessory proteins independently cause HIV-1-induced T cell cytopathicity and cell cycle arrest, Proc Natl Acad Sci U S A 103 (2006) 3369-3374.

[3] J. Wang, J.M. Shackelford, C.R. Casella, et al., The Vif accessory protein alters the cell cycle of human immunodeficiency virus type 1 infected cells, Virology 359 (2007) 243-252.

[4] X. Yu, Y. Yu, B. Liu, et al., Induction of APOBEC3G ubiquitination and degradation by an HIV-1 Vif-Cul5-SCF complex, Science 302 (2003) 1056-1060.

[5] S.P. Goff, Death by deamination: a novel host restriction system for HIV-1, Cell 114 (2003) 281-283.

[6] J.L. DeHart, A. Bosque, R.S. Harris, V. Planelles, Human immunodeficiency virus type 1 Vif induces cell cycle delay via recruitment of the same E3 ubiquitin ligase complex that targets APOBEC3 proteins for degradation, J Virol 82 (2008) 9265-9272.

[7] T. Izumi, K. Io, M. Matsui, et al., HIV-1 viral infectivity factor interacts with TP53 to induce G2 cell cycle arrest and positively regulate viral replication, Proc Natl Acad Sci U S A 107 (2010) 20798-20803.

[8] K. Zhao, J. Du, Y. Rui, et al., Evolutionarily conserved pressure for the existence of distinct G2/M cell cycle arrest and A3H inactivation functions in HIV-1 Vif, Cell Cycle 14 (2015) 838-847.

[9] E.J. Greenwood, N.J. Matheson, K. Wals, et al., Temporal proteomic analysis of HIV infection reveals remodelling

of the host phosphoproteome by lentiviral Vif variants, Elife 5 (2016).

[10] Y. Shi, Assembly and structure of protein phosphatase 2A, Sci China C Life Sci 52 (2009) 135-146.

[11] A. Mehle, J. Goncalves, M. Santa-Marta, M. McPike, D. Gabuzda, Phosphorylation of a novel SOCS-box regulates assembly of the HIV-1 Vif-Cul5 complex that promotes APOBEC3G degradation, Genes Dev 18 (2004) 2861-2866.

[12] Y. Yu, Z. Xiao, E.S. Ehrlich, X. Yu, X.F. Yu, Selective assembly of HIV-1 Vif-Cul5-ElonginB-ElonginC E3 ubiquitin ligase complex through a novel SOCS box and upstream cysteines, Genes Dev 18 (2004) 2867-2872.

[13] Y. Matsui, K. Shindo, K. Nagata, et al., Defining HIV-1 Vif residues that interact with CBFbeta by site-directed mutagenesis, Virology 449 (2014) 82-87.

[14] S.S. Margolis, J.A. Perry, C.M. Forester, et al., Role for the PP2A/B56delta phosphatase in regulating 14-3-3 release from Cdc25 to control mitosis, Cell 127 (2006) 759-773.

[15] D.J. Salamango, T. Ikeda, S.A. Moghadasi, et al., HIV-1 Vif Triggers Cell Cycle Arrest by Degrading Cellular PPP2R5 Phospho-regulators, Cell Rep 29 (2019) 1057-1065 e1054.

[16] L. Ronsard, R. Raja, V. Panwar, et al., Genetic and functional characterization of HIV-1 Vif on APOBEC3G degradation: First report of emergence of B/C recombinants from North India, Sci Rep 5 (2015) 15438.

[17] K. Reddy, M. Ooms, M. Letko, et al., Functional characterization of Vif proteins from HIV-1 infected patients with different APOBEC3G haplotypes, AIDS 30 (2016) 1723-1729.

[18] S.E. Guerra-Palomares, P.G. Hernandez-Sanchez, M.A. Esparza-Perez, et al., Molecular Characterization of Mexican HIV-1 Vif Sequences, AIDS Res Hum Retroviruses 32 (2016) 290-295.

Figure 1

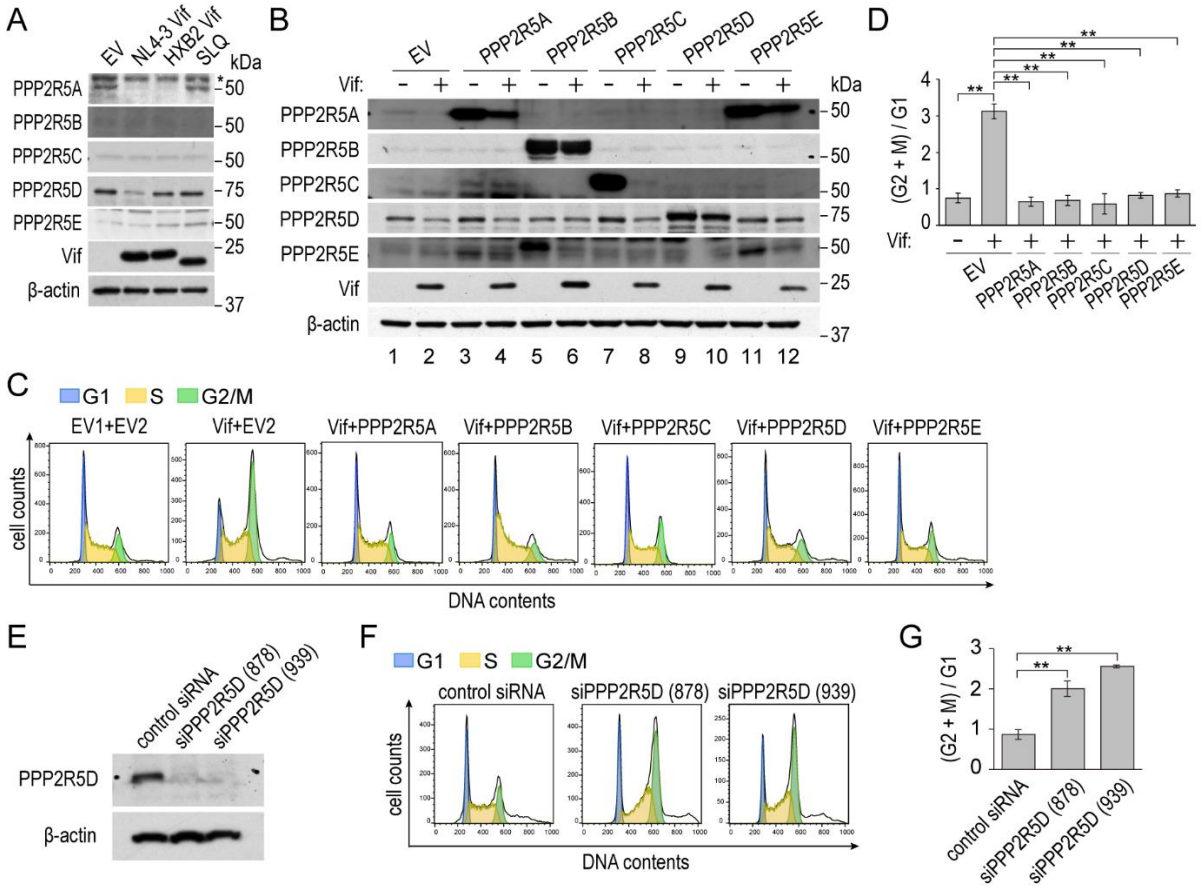
A
EV
NL4-3 Vif
HXB2 Vif
SLQ
kDa
PPP2R5A
PPP2R5B
PPP2R5C
PPP2R5D
PPP2R5E
Vif
β-actin
B
EV
PPP2R5A
PPP2R5B
PPP2R5C
PPP2R5D
PPP2R5E
Vif:
kDa
Vif
β-actin
1 2 3 4 5 6 7 8 9 10 11 12
D
(G2 + M) / G1
Vif:
EV
PPP2R5A
PPP2R5B
PPP2R5C
PPP2R5D
PPP2R5E
C
G1
S
G2/M
EV1+EV2
Vif+EV2
Vif+PPP2R5A
Vif+PPP2R5B
Vif+PPP2R5C
Vif+PPP2R5D
Vif+PPP2R5E
cell counts
DNA contents
E
control siRNA
siPPP2R5D (878)
siPPP2R5D (939)
PPP2R5D
β-actin
F
G1
S
G2/M
control siRNA
siPPP2R5D (878)
siPPP2R5D (939)
cell counts
DNA contents
G
(G2 + M) / G1
control siRNA
siPPP2R5D (878)
siPPP2R5D (939)

Figure 2

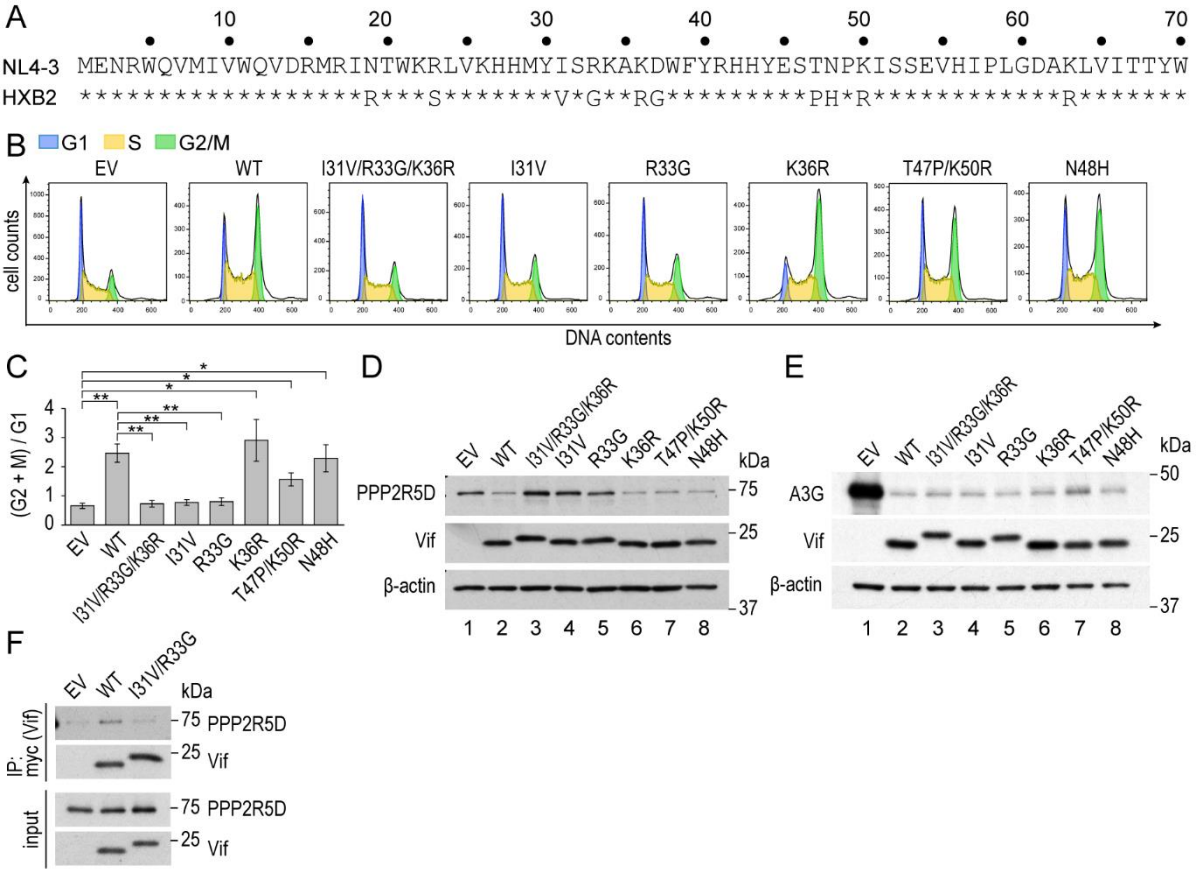
A
10
20
30
40
50
60
70
NL4-3 MENRWQVMIVWQVDRMRINTWKRLVKHHMYISRKAKDWFYRHHYESTNPKISSEVHIPLGDAKLVITTYW
HXB2 ********************R***S*******V*G**RG*********PH*R***********R*******
B
G1
S
G2/M
EV
WT
I31V/R33G/K36R
I31V
R33G
K36R
T47P/K50R
N48H
cell counts
DNA contents
C
(G2 + M) / G1
EV
WT
I31V/R33G/K36R
I31V
R33G
K36R
T47P/K50R
N48H
D
kDa
PPP2R5D
Vif
β-actin
75
25
37
1 2 3 4 5 6 7 8
E
kDa
A3G
Vif
β-actin
50
25
37
1 2 3 4 5 6 7 8
F
EV
WT
I31V/R33G
kDa
IP: myc (Vif)
PPP2R5D
Vif
input
PPP2R5D
Vif
75
25
75
25

Figure 3

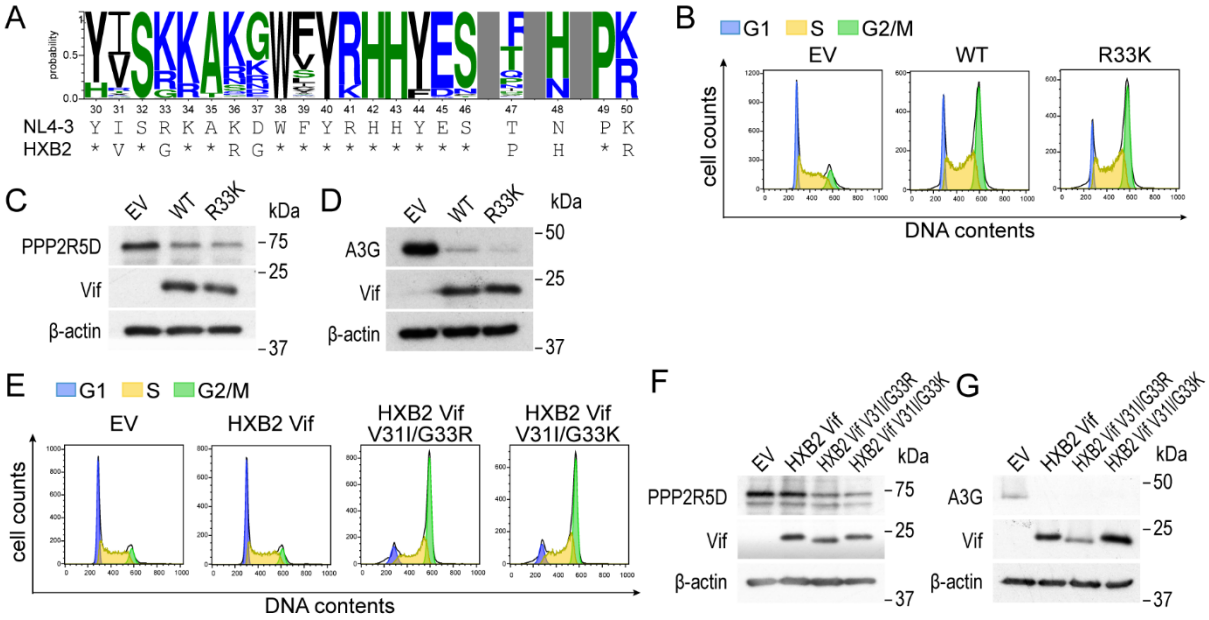
A
probability
30 31 32 33 34 35 36 37 38 39 40 41 42 43 44 45 46 47 48 49 50
NL4-3 Y I S R K A K D W F Y R H H Y E S T N P K
HXB2 * V * G * * R G * * * * * * * * * P H * R
B
G1 S G2/M
EV WT R33K
cell counts
DNA contents
C
EV WT R33K kDa
PPP2R5D
Vif
β-actin
75
25
37
D
EV WT R33K kDa
A3G
Vif
β-actin
50
25
37
E
G1 S G2/M
EV
HXB2 Vif
HXB2 Vif V31I/G33R
HXB2 Vif V31I/G33K
cell counts
DNA contents
F
EV HXB2 Vif HXB2 Vif V31I/G33R HXB2 Vif V31I/G33K kDa
PPP2R5D
Vif
β-actin
75
25
37
G
EV HXB2 Vif HXB2 Vif V31I/G33R HXB2 Vif V31I/G33K kDa
A3G
Vif
β-actin
50
25
37

Figure 4

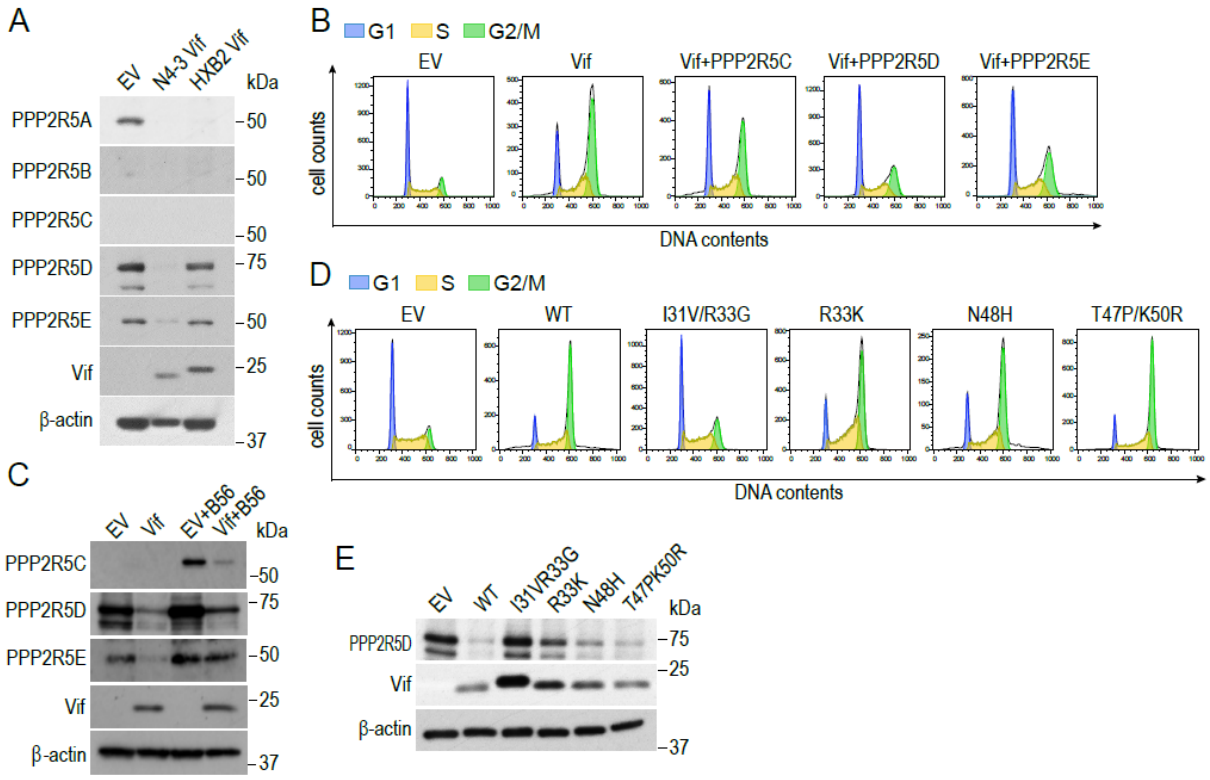
A
EV
N4-3 Vif
HXB2 Vif
kDa
PPP2R5A
PPP2R5B
PPP2R5C
PPP2R5D
PPP2R5E
Vif
β-actin
50
50
50
75
50
25
37
B
G1
S
G2/M
EV
Vif
Vif+PPP2R5C
Vif+PPP2R5D
Vif+PPP2R5E
cell counts
DNA contents
C
EV
Vif
EV+B56
Vif+B56
kDa
PPP2R5C
PPP2R5D
PPP2R5E
Vif
β-actin
50
75
50
25
37
D
G1
S
G2/M
EV
WT
I31V/R33G
R33K
N48H
T47P/K50R
cell counts
DNA contents
E
EV
WT
I31VR33G
R33K
N48H
T47PK50R
kDa
PPP2R5D
Vif
β-actin
75
25
37

Supplementary Material

Critical role of PP2A-B56 family protein degradation in HIV-1 Vif mediated G2 cell cycle arrest

Kayoko Nagata, Keisuke Shindo, Yusuke Matsui, Kotaro Shirakawa and Akifumi Takaori-Kondo

Department of Hematology and Oncology, Graduate School of Medicine, Kyoto University

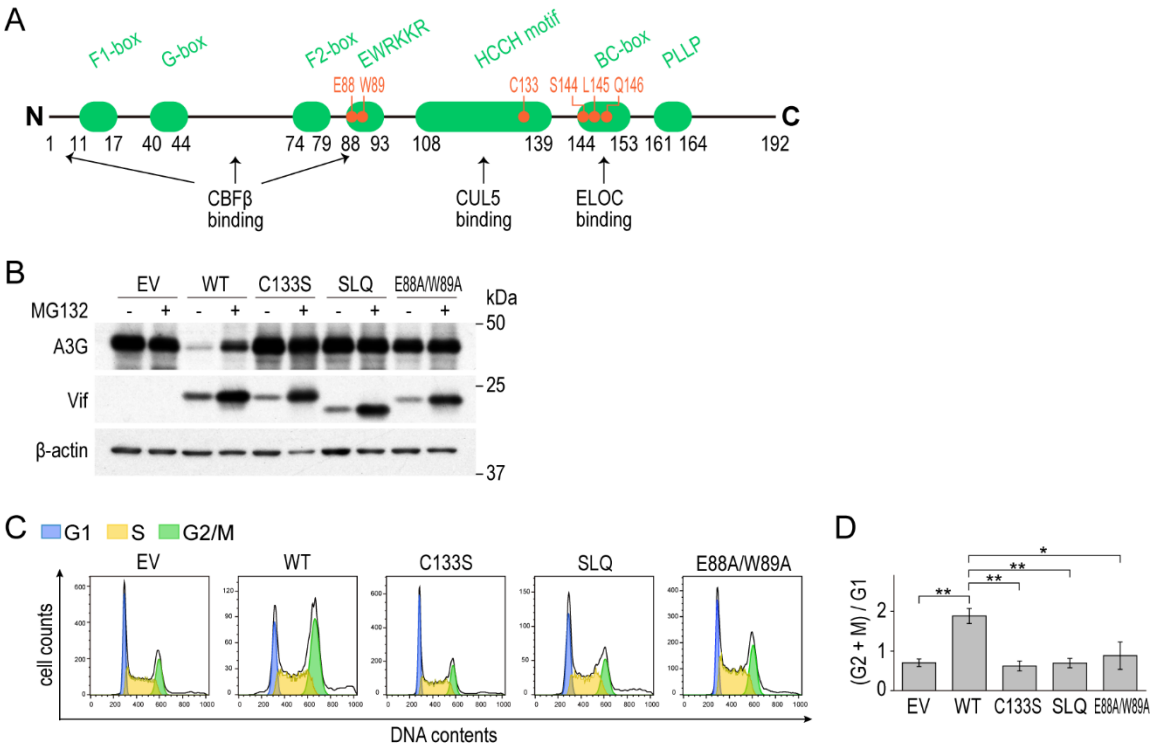

Supplementary Figure 1. The formation of the Vif-E3 ubiquitin ligase complex is required for Vif-mediated cell cycle arrest. (A) Schematic depicting of conserved Vif residues and binding partners. (B) Validation of amino acid substitutions that impair the ubiquitin ligase activity against APOBEC3G. 293T cells were transfected with expression vectors for APOBEC3G and Vif wild type (WT) or indicated mutant, or empty vector (EV) as control, cultured with MG132 or dimethyl sulfoxide as control, harvested and analyzed by immunoblotting. (C) Representative histogram for 293T cells transfected with indicated vectors. (D) Bar chart represents the (G2+M)/G1 ratios from three independent experiments in (C). Asterisks indicate statistical significances (*: P<0.05, **: P<0.01).

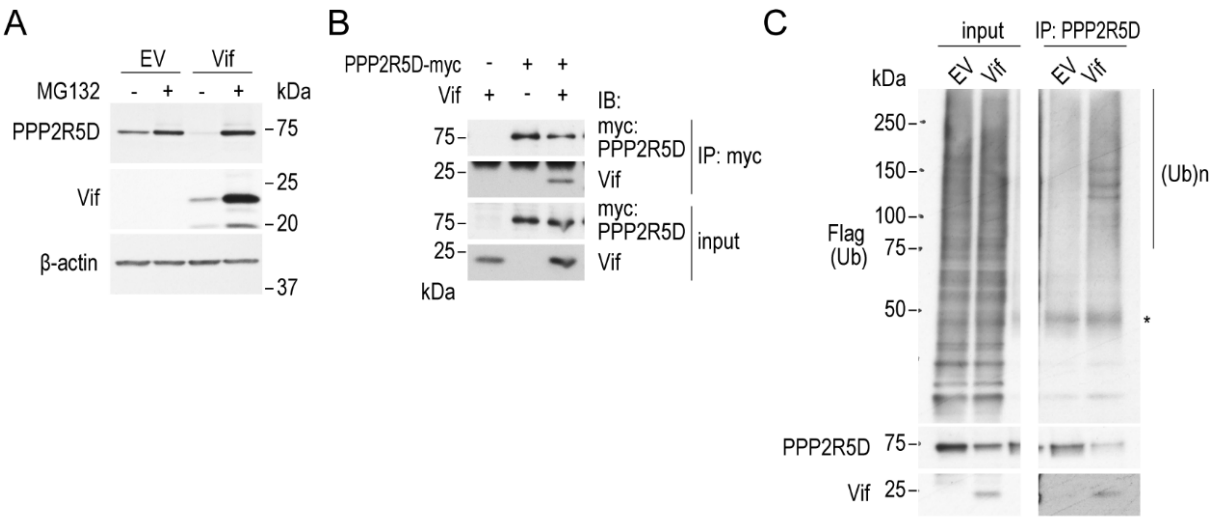

Supplementary Figure 2. PPP2R5D is a substrate of the NL4-3 Vif-E3 ubiquitin ligase complex. (A) Vif-mediated PPP2R5D downregulation is proteasome-dependent. 293T cells were transfected with the NL4-3 Vif expression vector or EV, treated with MG132 or dimethyl sulfoxide as control, and then analyzed for PPP2R5D protein levels by immunoblotting. (B) Co-immunoprecipitation of Vif with PPP2R5D. 293T cells were transfected with expression vectors for NL4-3 Vif and myc-tagged PPP2R5D, lysed with co-IP buffer, and immunoprecipitated with anti-myc antibody. Bound proteins were analyzed by immunoblotting with indicated antibodies. (C) Ubiquitination of PPP2R5D by NL4-3 Vif. 293T cells were transfected with expression vectors for Flag-tagged ubiquitin and NL4-3 Vif or EV, treated with MG132, and immunoprecipitated with antibodies for PPP2R5D. Bound proteins were analyzed by immunoblotting with indicated antibodies. The bands indicated by asterisk are heavy chains of the antibody used for immunoprecipitation.